Procedia Computer Science
Volume 51, 2015, Pages 905–913
ICCS 2015 International Conference On Computational Science

Shape Optimization of Trawl-Doors Using Variable-Fidelity Models and Space Mapping

Ingi M. Jonsson[1*], Leifur Leifsson[1,2†], Slawomir Koziel[1‡],
Yonatan A. Tesfahunegn[1§], and Adrian Bekasiewicz[1**]
[1]*Reykjavik University, Reykjavik, Iceland*
[2]*Iowa State University, Ames, Iowa, USA*
ingij10@ru.is, leifur@iastate.edu, koziel@ru.is, yonatant@ru.is, bekasiewicz@ru.is

Abstract
Trawl-doors have a large influence on the fuel consumption of fishing vessels. Design and optimization of trawl-doors using computational models are key factors in minimizing the fuel consumption. This paper presents an efficient optimization algorithm for the design of trawl-door shapes using computational fluid dynamic models. The approach is iterative and uses variable-fidelity models and space mapping. The algorithm is applied to the design of a multi-element trawl-door, involving four design variables controlling the angle of attack and the slat position and orientation. The results demonstrate that a satisfactory design can be obtained at a cost of a few iterations of the algorithm. Compared with direct optimization of the high-fidelity model and local response surface surrogate models, the proposed approach requires 79% less computational time while, at the same time, improving the design significantly (over 12% increase in the lift-to-drag ratio).

Keywords: Trawl-doors, hydrodynamics, surrogate-based optimization, computational fluid dynamics, space mapping.

1 Introduction

A major part of the fuel of fishing vessels is spent during trawling (often over 60%). Therefore, there is a great incentive to reduce the drag of the fishing gear. The main parts of a fishing gear assembly are the net, a pair of trawl-doors, and a cable extending from the trawl-doors to the boat and the net (see Fig. 1(a)). The role of the trawl-doors is to keep the net open during the trawling operation Fig. 1(b). The trawl-doors can be responsible for roughly 10-30% of the total drag of the entire assembly (Garner, 1967; Haraldsson, 1996; Jonsson *et al.*, 2012; Jonsson *et al.*, 2013). Therefore, significant fuel consumption savings may be possible by careful design and optimization of trawl-doors.

* Engineering Optimization & Modeling Center, School of Science and Engineering
† Department of Aerospace Engineering
‡ Engineering Optimization & Modeling Center, School of Science and Engineering
§ Engineering Optimization & Modeling Center, School of Science and Engineering
** Engineering Optimization & Modeling Center, School of Science and Engineering

Selection and peer-review under responsibility of the Scientific Programme Committee of ICCS 2015

doi:10.1016/j.procs.2015.05.223

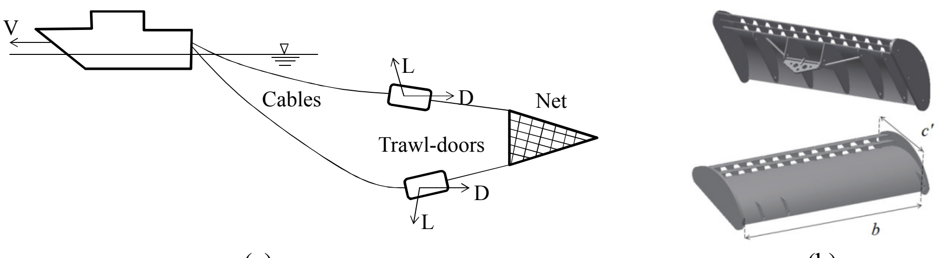

Figure 1: A schematic of a fishing vessel with trawling gear illustrating (a) the main parts of the fishing gear, and (b) a typical trawl-door with leading-edge two slats (Leifsson *et al*., 2015).

Recently, a design optimization approach for trawl-doors using accurate, high-fidelity computational fluid dynamics (CFD) models has been introduced (Leifsson *et al*., 2014; Leifsson *et al*., 2015), which exploits an iterative scheme with local response surface approximation (RSA) models of the expensive CFD trawl-door model constructed in each iteration. The RSA models are constructed using CFD data sparsely sampled in the vicinity of the current design, and a low-order polynomial approximation (to reduce the influence of the CFD model numerical noise on the optimization, as well as minimizing the number of required data samples). The size of the vicinity (i.e., the RSA model domain) is automatically adjusted in each iteration based on the performance of the model, more specifically, on the quality of the prediction given by the model as compared to the actual changes of the trawl-door performance metrics verified by the CFD simulation. The adjustment scheme is governed by a conventional trust region framework.

In this paper, we accelerate the design optimization by using physics-based surrogate models. In particular, the computational cost is shifted from the accurate high-fidelity CFD model to a suitably corrected low-fidelity model, which is constructed using space mapping and a coarse-discretization CFD model with relaxed convergence criteria. Since the low-fidelity model is based on the same physics as the high-fidelity one, less high-fidelity data is necessary to construct the surrogate when compared with the RSA models. This work demonstrates that the proposed method can yield significant computational savings compared to conventional approaches.

2 Problem Formulation

We consider multi-element trawl-door configurations that have a leading-edge slat and a trailing-edge flap as shown in Fig. 2. The overall objective is to optimize the shape and configuration of the elements (other components of the trawling gear are not considered). The drag coefficient is minimized for a given lift coefficient (to ensure sufficient opening of the net). In particular, the optimization problem is formulated as

$$\min C_d(\boldsymbol{x}) \tag{1}$$

subject to

$$C_l(\boldsymbol{x}) \geq C_l^* \tag{2}$$

where C_d is the drag coefficient (a non-dimensional form of the trawl-door drag), C_l is the lift coefficient, C_l^* is the target lift coefficient, and $\boldsymbol{x}$ is the vector of design variables.

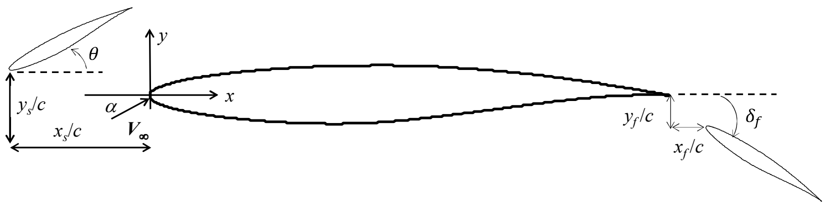

Figure 2: A section cut of a trawl-door with airfoil shaped elements, including a leading-edge slat and a trailing-edge flap (Leifsson *et al.*, 2015).

In this work, only the position and inclination of the elements are designable parameters. The shapes of the elements are fixed. The operating condition (defined by the speed, V_∞) is also fixed during the optimization. We can write the design variable vector as

$$\boldsymbol{x} = [x_s/c \quad y_s/c \quad \theta \quad x_f/c \quad y_f/c \quad \delta_f \quad \alpha]^T \tag{3}$$

where x_s/c is the slat leading-edge position on the x-axis, y_s/c is the slat leading-edge position on the y-axis, θ is the slat inclination relative to the x-axis, x_f/c is the flap leading-edge position on the x-axis, y_f/c is the flap leading-edge position on the y-axis, δ_f is the flap inclination relative to the x-axis, α is the angle of attack, and c is the length of the main element (c = 1 in this study). Bounds are prescribed on the design variables, i.e., $\boldsymbol{l} \leq \boldsymbol{x} \leq \boldsymbol{u}$ where $\boldsymbol{l}$ and $\boldsymbol{u}$ are lower and upper bounds, respectively.

The above problem can be re-written in the following form

$$\boldsymbol{x}^* = \arg\min_{\boldsymbol{x}} H(\boldsymbol{f}(\boldsymbol{x})), \tag{4}$$

where $\boldsymbol{f}$ is the high-fidelity model response, typically representing hydrodynamic forces such as lift and drag, and H is the objective function. In this work, we have $\boldsymbol{f}(\boldsymbol{x}) = [C_{l.f}(\boldsymbol{x}) \; C_{d.f}(\boldsymbol{x})]^T$, where $C_{l.f}$ and $C_{d.f}$ are the lift and drag coefficients obtained by a high-fidelity model. For drag minimization, the objective function takes the form $H(\boldsymbol{f}(\boldsymbol{x})) = C_{d.f}(\boldsymbol{x})$. The design constraint is denoted $C(\boldsymbol{f}(\boldsymbol{x})) = c_1(\boldsymbol{f}(\boldsymbol{x})) = C^*_{l.f} - C^*_{l.f}(\boldsymbol{x}) \leq 0$.

3 Optimization Using Space Mapping

The objective of this work is to solve the problem (4) using as few high-fidelity model evaluations, $\boldsymbol{f}(\boldsymbol{x})$, as possible. To achieve this, we use surrogate-based optimization (SBO) (Queipo *et al.*, 2005; Forrester and Keane, 2009; Koziel, Echeverra-Ciaurri, and Leifsson, 2011; Koziel and Leifsson, 2013). In SBO, the computational load is shifted from the high-fidelity model, $\boldsymbol{f}(\boldsymbol{x})$, to a surrogate model, $\boldsymbol{s}(\boldsymbol{x})$, which is a cheap representation of the high-fidelity one. In this work, the surrogate model is constructed from a low-fidelity model, $\boldsymbol{c}(\boldsymbol{x})$, which is corrected by using space mapping (SM) (Bandler *et al.*, 2004; Koziel and Leifsson, 2012).

A generic SM algorithm (Koziel and Leifsson, 2012) produces a sequence $\boldsymbol{x}^{(i)}$, i = 0, 1, …, of approximate solutions to (4) (here, $\boldsymbol{x}^{(0)}$ is the initial design) as

$$\boldsymbol{x}^{(i+1)} = \arg\min_{\boldsymbol{x}} H(\boldsymbol{s}^{(i)}(\boldsymbol{x})), \tag{5}$$

where $\boldsymbol{s}^{(i)}(\boldsymbol{x}) = [C_{l.s}^{(i)}(\boldsymbol{x}) \; C_{d.s}^{(i)}(\boldsymbol{x})]^T$ is a surrogate model at iteration i. The surrogate model is a composition of the low-fidelity model and simple, usually linear, transformations (or mappings). The generic SM surrogate model can be written as $s(\boldsymbol{x},\boldsymbol{p})$, where $\boldsymbol{p}$ represents model parameters. The surrogate at iteration i is then

$$\boldsymbol{s}^{(i)}(\boldsymbol{x}) = s(\boldsymbol{x}, \boldsymbol{p}^{(i)}), \tag{6}$$

with the parameters $\boldsymbol{p}^{(i)}$ determined through a so-called parameter extraction process to minimize the misalignment between the surrogate and the high-fidelity model at some or all previous iterations points, where the high-fidelity data is already available. Parameter extraction is, in general, solved as a nonlinear minimization problem of the form

$$\boldsymbol{p}^{(i)} = \arg\min_{\boldsymbol{p}} \sum_{k=0}^{i} w_{i.k} \| \boldsymbol{f}(\boldsymbol{x}^{(k)}) - \boldsymbol{s}(\boldsymbol{x}^{(k)}, \boldsymbol{p}) \|^2, \tag{7}$$

where $w_{i.k}$ are weighting factors determining the influence of previous iteration points on the SM model parameters. Two widely used setups are $w_{i.k} = 1$ for all i and k, and $w_{i.k} = 1$ for $k = i$ and $w_{i.k} = 0$ for $k \neq i$. In the latter case, the model only depends on the most recent SM iteration.

Examples of SM surrogate models include input SM, where $\boldsymbol{s}(\boldsymbol{x},\boldsymbol{p}) = \boldsymbol{s}(\boldsymbol{x},\boldsymbol{q}) = \boldsymbol{c}(\boldsymbol{x} + \boldsymbol{q})$ (parameter shift), or $\boldsymbol{s}(\boldsymbol{x},\boldsymbol{p}) = \boldsymbol{s}(\boldsymbol{x},\boldsymbol{B},\boldsymbol{q}) = \boldsymbol{c}(\boldsymbol{B}\boldsymbol{x} + \boldsymbol{q})$ (parameter shift and scaling), and output SM, with $\boldsymbol{s}(\boldsymbol{x},\boldsymbol{p}) = \boldsymbol{s}(\boldsymbol{x},\boldsymbol{A}) = \boldsymbol{A} \cdot \boldsymbol{c}(\boldsymbol{x})$ (multiplicative response correction) or $\boldsymbol{s}(\boldsymbol{x},\boldsymbol{p}) = \boldsymbol{s}(\boldsymbol{x},\boldsymbol{d}) = \boldsymbol{c}(\boldsymbol{x}) + \boldsymbol{d}$ (additive response correction). In this work, we use both multiplicative and additive response correction (Koziel and Leifsson, 2012):

$$\boldsymbol{s}^{(i)}(\boldsymbol{x}) = \boldsymbol{A}^{(i)} \circ \boldsymbol{c}(\boldsymbol{x}) + \boldsymbol{D}^{(i)} + \boldsymbol{q}^{(i)} = [a_l^{(i)} C_{l.c}(\boldsymbol{x}) + d_l^{(i)} + q_l^{(i)} \quad a_d^{(i)} C_{d.c}(\boldsymbol{x}) + d_d^{(i)} + q_d^{(i)}]^T, \tag{8}$$

where ° denoted component-wise multiplication. The response correction parameters $\boldsymbol{A}^{(i)}$ and $\boldsymbol{D}^{(i)}$ are obtained by solving

$$[\boldsymbol{A}^{(i)}, \boldsymbol{D}^{(i)}] = \arg\min_{[\boldsymbol{A},\boldsymbol{D}]} \sum_{k=0}^{i} \| \boldsymbol{f}(\boldsymbol{x}^{(k)}) - \boldsymbol{A} \circ \boldsymbol{c}(\boldsymbol{x}^{(k)}) + \boldsymbol{D} \|^2, \tag{9}$$

i.e., the response scaling is supposed to (globally) improve the matching for all previous iteration points. The additive response correction term $\boldsymbol{q}^{(i)}$ is defined as

$$\boldsymbol{q}^{(i)} = \boldsymbol{f}(\boldsymbol{x}^{(i)}) - [\boldsymbol{A}^{(i)} \circ \boldsymbol{c}(\boldsymbol{x}^{(i)}) + \boldsymbol{D}^{(i)}], \tag{10}$$

i.e., it ensures a perfect matching between the surrogate and the high-fidelity model at the current design $\boldsymbol{x}^{(i)}$, $\boldsymbol{s}^{(i)}(\boldsymbol{x}^{(i)}) = \boldsymbol{f}(\boldsymbol{x}^{(i)})$ (the so-called zero-order consistency condition).

Both $\boldsymbol{A}^{(i)}$, $\boldsymbol{D}^{(i)}$ and $\boldsymbol{q}^{(i)}$ can be calculated analytically so that there is no need to carry out nonlinear-minimization-like parameter extraction process (9). The term $\boldsymbol{q}^{(i)}$ can be calculated using (10). Terms $\boldsymbol{A}^{(i)}$ and $\boldsymbol{D}^{(i)}$ can be obtained as (Koziel and Leifsson, 2012)

$$\begin{bmatrix} a_l^{(i)} \\ d_l^{(i)} \end{bmatrix} = (\boldsymbol{C}_l^T \boldsymbol{C}_l)^{-1} \boldsymbol{C}_l^T \boldsymbol{F}_l, \qquad \begin{bmatrix} a_d^{(i)} \\ d_d^{(i)} \end{bmatrix} = (\boldsymbol{C}_d^T \boldsymbol{C}_d)^{-1} \boldsymbol{C}_d^T \boldsymbol{F}_d, \tag{11}$$

where

$$\boldsymbol{C}_l = \begin{bmatrix} C_{l.c}(\boldsymbol{x}^{(0)}) & C_{l.c}(\boldsymbol{x}^{(1)}) & \cdots & C_{l.c}(\boldsymbol{x}^{(i)}) \\ 1 & 1 & \cdots & 1 \end{bmatrix}^T, \quad \boldsymbol{F}_l = \begin{bmatrix} C_{l.f}(\boldsymbol{x}^{(0)}) & C_{l.f}(\boldsymbol{x}^{(1)}) & \cdots & C_{l.f}(\boldsymbol{x}^{(i)}) \\ 1 & 1 & \cdots & 1 \end{bmatrix}^T, \tag{12}$$

$$\boldsymbol{C}_d = \begin{bmatrix} C_{d.c}(\boldsymbol{x}^{(0)}) & C_{d.c}(\boldsymbol{x}^{(1)}) & \cdots & C_{d.c}(\boldsymbol{x}^{(i)}) \\ 1 & 1 & \cdots & 1 \end{bmatrix}^T, \quad \boldsymbol{F}_d = \begin{bmatrix} C_{d.f}(\boldsymbol{x}^{(0)}) & C_{d.f}(\boldsymbol{x}^{(1)}) & \cdots & C_{d.f}(\boldsymbol{x}^{(i)}) \\ 1 & 1 & \cdots & 1 \end{bmatrix}^T, \quad (13)$$

which is a least-square optimal solution to the linear regression problem $\boldsymbol{C}_l a_l^{(i)} + d_l^{(i)} = \boldsymbol{F}_l$ and $\boldsymbol{C}_d a_d^{(i)} + d_d^{(i)} = \boldsymbol{F}_d$, equivalent to (10). Note that the matrices $\boldsymbol{C}_l^T\boldsymbol{C}_l$ and $\boldsymbol{C}_d^T\boldsymbol{C}_d$ are non-singular for $i > 1$. For $i = 1$ only the multiplicative correction with $\boldsymbol{A}^{(i)}$ components are used, which can be calculated in a similar way.

4 Variable-Fidelity Modeling

This section describes the high- and low-fidelity models used in this study. We use a two-dimensional computational fluid dynamics (CFD) model to describe the flow behavior of the trawl-door. A two-dimensional CFD model can give a good description of the main flow characteristics of high-aspect ratio wings and is considered to be sufficient to demonstrate the proposed optimization algorithm. A full three-dimensional model should be used for detailed analysis and design of a trawl-door to capture the flow field more accurately.

4.1 High-Fidelity Model

The flow is assumed two-dimensional, steady, incompressible, and viscous. The Reynolds-averaged Navier-Stoke (RANS) equations are taken to be the governing equations with Menter's k-ω SST turbulence model (refer to Tannehill *et al*. (1997) for further details).

The farfield is configured in a box-topology where the trawl-door geometry is placed in the center of the box. The main element leading edge (LE) is placed as the origin, with the farfield extending 100 chord lengths away from the origin in every direction (Fig. 3(a)). The choice of using a box-topology in this case is because it is simple to implement. Other shapes can be used, such as a circle. However, the farfield needs to be far enough from the trawl-door so the boundary conditions (a constant velocity inlet and a constant pressure outlet) remain consistent in the flow solution.

We use an unstructured triangular grid where the elements are clustered around the trawl-door geometry, growing in size as they move away from the origin. The maximum element size on the geometry is set to 0.025% of the chord length and the maximum element size in domain away from the trawl-door is 10 times the chord length. These particular sizes are the results of parametric studies where the flow is analyzed to make sure to capture the main characteristic flow features. Moreover, in order to capture the viscous boundary layer well, a prismatic inflation layer is extruded from all surfaces. The initial layer height is chosen so that $y^+ < 1$. The mesh is generated with ICEM CFD (2012). An example mesh is shown in Figs. 3(b) and 3(c).

Numerical fluid flow simulations are performed using the commercial computer code FLUENT (2012). The flow solver is coupled velocity-pressure-based formulation. The spatial discretization schemes are second order for all flow variables and the gradient information is found using the Green-Gauss node based method. Additionally, due to the complex flow conditions which are observed at high angle of attack a pseudo-transient option and high-order relaxation terms are used in order to get a stable converged solution. The residuals, which are the sum of the L^2 norms of all governing equations in each cell, are monitored and checked for convergence. The convergence criterion is such that a solution is considered to be converged if the residuals have dropped by six orders of magnitude, or the total number of iterations has reached 5,000.

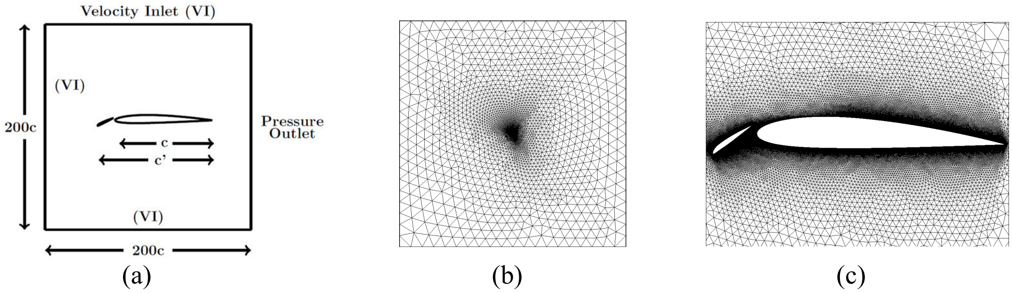

Figure 3: Two-dimensional CFD model: (a) the solution domain and boundary conditions, and an example two dimensional computational mesh, (b) the farfield, and (c) a close-up of the trawl-door surface.

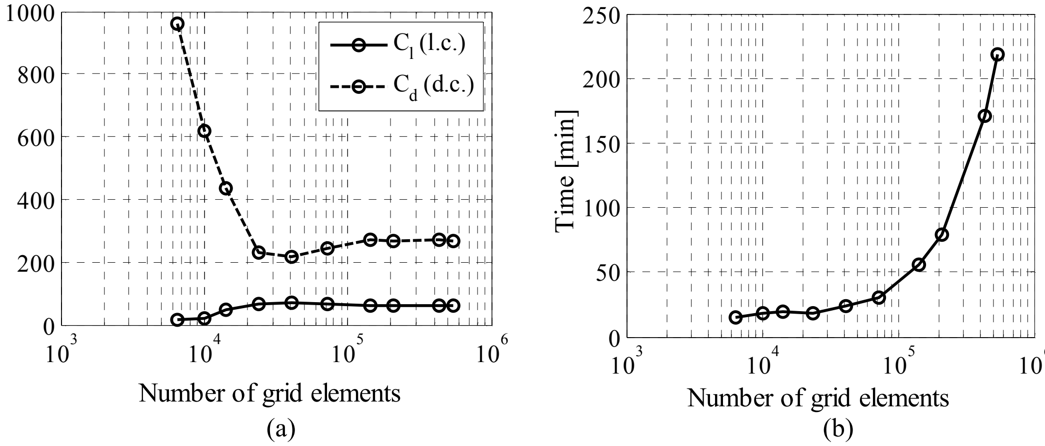

Figure 4: Grid convergence study using a two element airfoil (slat: NACA 3210, main element: NACA 2412) at $V_\infty = 2$ m/s, $Re = 2 \times 10^6$, $\alpha = 5°$: (a) lift and drag coefficients versus the number of grid elements, (b) the simulation time versus the number of grid elements.

A sufficiently fine enough mesh is found by carrying out a grid convergence study of a two element airfoil (slat: NACA 3210, main element: NACA 2412, see coordinates in Abbott and Von Doenhoff (1959), at speed $V_\infty = 2$ m/s, Reynolds number $Re = 2 \times 10^6$, and an angle of attack $\alpha = 5°$. The results are shown in Fig. 4 and reveal that around 517,000 grid elements are needed for convergence. The overall simulation time needed for one high-fidelity CFD simulation was around 171 minutes, executed on two Intel Xeon(R) X5660 2.8 GHz processors in parallel (5,000 solver iterations where required).

4.2 Low-Fidelity Model

The low-fidelity CFD model is the same as the high-fidelity one, but with a coarser mesh discretization and relaxed flow solver convergence criteria. In particular, based on the grid convergence study presented in Fig. 4, we select the low-fidelity model with about 15,000 elements. The maximum number of flow solver iterations is fixed 500. The resulting low-fidelity model is around 78 times faster on average than the high-fidelity model.

5 Numerical Example

5.1 Description

The trawl-door to be optimized has a main element shape of the NACA 2412 profile and a slat of the NACA 3210 profile, see Fig. 2. The NACA profiles are specifically designed for low-speed applications. The chord lengths of both elements are fixed, with the chord length of the slat (c_s) being 20% of the main element chord length (c). The operating speed is V_∞ = 2 m/s (which is a typical speed during trawling (Garner, 1967).

The objective is to minimize the section drag coefficient (C_d) subject to a constraint on the section lift coefficient ($C_l \geq 1.2$) as described in Section 2. The design variables are the x_s/c and y_s/c locations of the slat leading-edge with respect to the main element leading-edge, the angle incidence of the slat (θ) with respect to the main element chord line, and the angle of attack (α) of the assembly. The search domain is set as: $-0.35 \leq x/c \leq -0.17$, $-0.08 \leq y/c \leq 0.07$, $10 \leq \theta \leq 40$ deg, $5 \leq \alpha \leq 35$ deg. The initial design is $x/c = -0.2$, $y/c = -0.08$, $\theta = 25$ deg, and $\alpha = 8$ deg.

5.2 Results

The optimization results are shown in Table 1. The initial and optimized trawl-door shapes are shown in Fig. 5. The optimized design has $x/c = -0.200$, $y/c = -0.0633$, $\theta = 24.1$ deg, and $\alpha = 8.4$ deg, with $C_l = 1.20$ and $C_d = 0.0153$ giving a lift-to-drag ratio of 78.4. The SM optimizer required 14 high-fidelity model evaluations and 400 low-fidelity ones, yielding a total runtime of approximately 55 hours. The convergence history is shown in Fig. 6, where it can be seen that the initial design is infeasible but the optimizer quickly approach the lift constraint value and finally converges on the objective value change. Compared with our previous study of this particular problem using local surrogate model (Leifsson *et al.*, 2015), the SM mapping algorithm outperforms it by reducing the optimization cost by 79% while improving the design significantly.

Table 1: Comparison of SM optimization results with an approach using local surrogates.

	Previous study[#]	**Current study**	**Relative difference**
$(x/c)_{slat}$	−0.2289	−0.2000	–
$(y/c)_{slat}$	−0.0066	−0.0633	–
θ [deg]	20.4968	24.1111	–
α [deg]	8.2756	8.3745	–
C_l	1.1985	1.2002	0.1%
C_d	0.0174	0.0153	−13.7%
C_l/C_d	68.8793	78.4444	12.2%
Iterations	9	11	–
Evaluations	110	14/400[$]	–
CFD Runtime [hours]	≈262	≈55	−79.0%

[#] Data from Leifsson *et al.* (2015).
[$] High- and low-fidelity model evaluations.

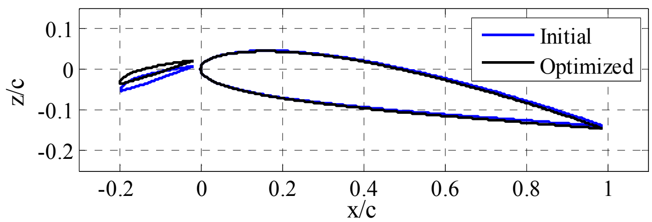

Figure 5: Initial and optimized trawl-door shapes. The flow is parallel to the *x*/*c*-axis.

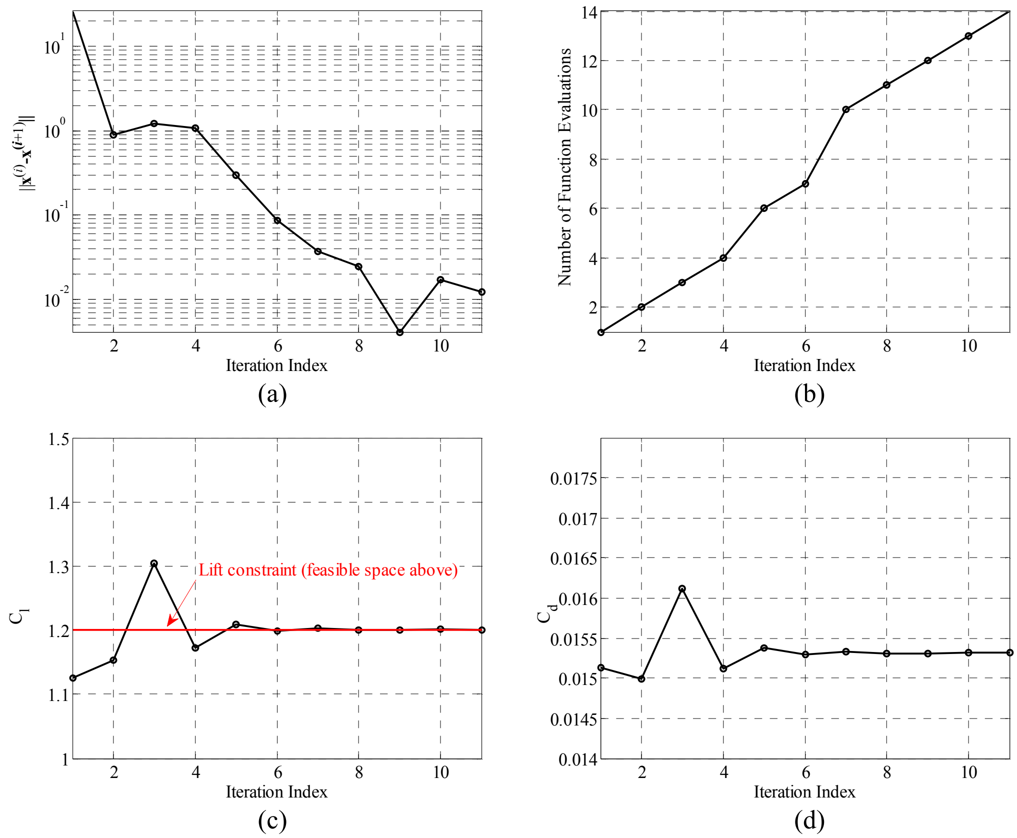

Figure 6: Optimization history: (a) argument convergence, (b) number of high-fidelity function evaluations, (c) evolution of the lift coefficient and the constraint bound, and (d) evolution of the drag coefficient.

6 Conclusion

A computationally efficient optimization methodology for the hydrodynamic design of multi-element trawl-door shapes using high-fidelity two-dimensional CFD models has been presented. Our approach exploits variable-fidelity models and space mapping for low-fidelity model correction. Numerical design studies of multi-element trawl-door shapes illustrate that satisfactory designs can be obtained at the cost of a few iterations of the algorithm.

References

Abbott, I.H., and Von Doenhoff, A.E. (1959) *Theory of Wing Sections*. Dover Publications, New York, New York, USA.

Bandler, J.W., Cheng, Q.S., Dakroury, S.A., Mohamed, A.S., Bakr, M.H., Madsen, K., and Søndergaard, J. (2004) Space mapping: the state of the art. *IEEE Trans. Microwave Theory Tech.*, 52, pp. 337−361.

Garner, J. (1967) *Botnvarpan og bunadur hennar*, Fiskifelag Islands, 1967.

Haraldsson, H.O. (1996) Fluid Dynamics Simulation of Fishing Gear. M.Sc. Thesis, University of Iceland.

FLUENT (2012), ver. 14.0, ANSYS Inc., Southpointe, 275 Technology Drive, Canonsburg, PA 15317.

Forrester, A.I.J., and Keane, A.J. (2009) Recent advances in surrogate-based optimization. *Progress in Aerospace Sciences*, Vol. 45, No. 1-3, pp. 50-79.

ICEM CFD (2012), ver. 14.0, ANSYS Inc., Southpointe, 275 Technology Drive, Canonsburg, PA 15317.

Jonsson, E., Leifsson, L., and Koziel, S. (2012) Trawl-Door Performance Analysis and Design Optimization with CFD. *2nd Int. Conf. on Simulation and Modeling Methodologies, Technologies, and Applications (SIMULTECH)*, Rome, Italy, July 28-31.

Jonsson, E., Hermannsson, E., Juliusson, M., Koziel, S., and Leifsson, L. (2013) Computational Fluid Dynamic Analysis and Shape Optimization of Trawl-Doors. *51st AIAA Aerospace Sciences Meeting including the New Horizons Forum and Aerospace Exposition*, Grapevine, Texas, January 7-10.

Koziel, S., Echeverra-Ciaurri, D., and Leifsson, L. (2011) Surrogate-based methods. In S. Koziel and X.S. Yang (Eds.) Computational Optimization, Methods and Algorithms, Series: Studies in Computational Intelligence, Springer-Verlag, pp. 33-60.

Koziel, S., and Leifsson, L. (2012) Knowledge-Based Airfoil Shape Optimization Using Space Mapping. *30th AIAA Applied Aerodynamics Conference*, New Orleans, Louisiana, June 25-28.

Koziel, S., and Leifsson, L. (2013) Surrogate-Based Aerodynamic Shape Optimization by Variable-Resolution Models. *AIAA Journal*, vol. 51, no. 1, pp. 94–106.

Leifsson, L., Koziel, S., Hermannsson, E., and Fakhraie, R. (2014) Trawl-Door Design Optimization by Local Surrogate Models. *55th AIAA/ ASMe/ASCE/AHS/SC Structures, Structural Dynamics, and Materials Conference*, National Harbor, Maryland, Jan. 13-17.

Leifsson, L., Hermannsson, E., and Koziel, S. (2015) Optimal shape design of multi-element trawl-doors using local surrogate models. *Journal of Computational Science*, doi: 10.1016/j.jocs.2015.01.006.

Tannehill, J.A., Anderson, D.A., and Pletcher, R.H. (1997) *Computational fluid mechanics and heat transfer*, 2nd edition. Taylor & Francis.

Queipo, N.V., Haftka, R.T., Shyy, W., Goel, T., Vaidyanathan, R., and Tucker, P.K. (2005) Surrogate-Based Analysis and Optimization. *Progress in Aerospace Sciences*, Vol. 41, No. 1, 2005, pp. 1-28.